Journal of Industrial and Engineering Chemistry 63 (2018) 33–40

Contents lists available at ScienceDirect

Journal of Industrial and Engineering Chemistry

journal homepage: www.elsevier.com/locate/jiec

Conjugated polymer nano-ellipsoids assembled with octanoic acid and their polyurethane nanocomposites with simultaneous thermal storage and antibacterial activity

Dabin Lee[a], Tae Joo Shin[b], Pil J. Yoo[c], Kyung Wha Oh[d,*], Juhyun Park[a,*]

[a] School of Chemical Engineering and Materials Science, Institute of Energy Converting Soft Materials, Chung-Ang University, Seoul 06974, Republic of Korea
[b] UNIST Central Research Facilities & School of Natural Science, Ulsan National Institute of Science and Technology (UNIST), Ulsan 44919, Republic of Korea
[c] School of Chemical Engineering and SKKU Advanced Institute of Nanotechnology (SAINT), Suwon 16419, Republic of Korea
[d] Department of Fashion Design, Chung-Ang University, Seoul 06974, Republic of Korea

ARTICLE INFO

Article history:
Received 11 October 2017
Received in revised form 22 January 2018
Accepted 27 January 2018
Available online 4 February 2018

Keywords:
Conjugated polymers
Nano-ellipsoids
Polyurethanes
Antibacterial
Thermal storage

ABSTRACT

We prepared conjugated polymer nano-ellipsoids (CPNs) via emulsification of chloroform phase using the octanoic acid (OA) in dimethyl formamide (DMF), followed by the removal of chloroform by heating. The resulting CPN DMF solutions were thoroughly mixed with polyurethane (PU) DMF solutions to form composite films upon solvent removal, with uniformly distributed CPNs due to hydrogen bonds between PU matrix and the CPNs. Superior photothermal and antibacterial properties of the PU:CPN composite films were observed, presenting the usefulness of CPNs as an efficient light harvester and thermal storage material, and the OA as an antibacterial material for multifunctional fiber applications.

Introduction

Functional fibers with thermal storage and antibacterial properties have received considerable attention for use in future fiber technologies. For example, heat loss from the human body can be reduced by enhancing thermal insulation through trapped air in hollow fibers [1,2] or through reflecting radiation heat upon the application of metal coatings on fibers used in clothing [3]. Further, far-infrared ceramic nanoparticles, such as zirconium carbide nanoparticles, embedded in fibers effectively absorb 95% of the solar energy impinging on their surface and convert the energy to heat with a thermal emissivity above 90% or reflect the heat generated by the human body, thereby demonstrating efficient thermal storage capacity [4–8]. In addition, phase-change materials embedded in fibers can emit thermal energy upon phase change with decreasing temperature, thus providing warmth [9]. On the other hand, bacteria or fungi can proliferate in fibers, deteriorating the properties of the fibers and generating unpleasant odor. To hinder the aging of fibers by bacteria or fungi, inorganic antimicrobial materials such as silver, copper and zinc and zeolites have been added into, coated onto, or composited with fiber materials [10,11]. These inorganic antimicrobial materials diffuse through the cell membranes of bacteria or fungi as metal ions (Ag^{+}, Zn^{2+}, Cu^{2+}) and are adsorbed on the thiol groups of Cysteine in cellular enzymes, thereby decreasing the enzyme activity and ultimately killing the cells. Furthermore, active oxygen radicals that can destroy the molecular structures of bacteria can be generated by catalytic reactions of the metals. Moreover, the high specific surface area of porous zeolites allows for enhanced adsorption of bacteria, and consequently, effective removal of bacteria.

This letter presents the fabrication of multifunctional nanocomposites that have both thermal storage and antimicrobial properties, which have rarely been reported. Recently, conjugated polymer nanoparticles (CPNs) have been highlighted as promising photothermal, photoacoustic, and photocatalytic materials [12–17]. As organic semiconductors, conjugated polymers with low bandgaps can absorb a broad range of solar light, including visible and near infrared light, as widely demonstrated for polymeric photovoltaic devices. When dispersed in aqueous media as nanoparticles, they can effectively absorb energy and emit heat. Furthermore, CPNs can induce an increase in medium temperature upon static laser irradiation to kill cancer cells [12–14], or generate acoustic waves upon pulsed laser irradiation followed by the fluctuation of local densities [15,16], which should be useful for both photothermal therapy and photoacoustic imaging. As an

* Corresponding authors.
E-mail addresses: kwhaoh@cau.ac.kr (K.W. Oh), jpark@cau.ac.kr (J. Park).

https://doi.org/10.1016/j.jiec.2018.01.035
1226-086X/

excellent light harvester, CPNs can absorb a vast quantity of solar energy and transfer this energy for photocatalytic reactions as recently reviewed [17,18]. Thus, CPNs may contribute to thermal storage by absorbing solar energy and emitting heat when they are composited with fiber materials. As for the antimicrobial material properties, we noticed the antimicrobial activity of fatty acids. For instance, saturated or unsaturated fatty acids with a carboxyl group (−COOH) at one end, such as scleropyric acid (natural C18 fatty acid), 2-hexadecynoic acid, and linoleic acid (18:2), showed antiplasmodial, antibacterial, and antifungal activities, respectively [19]. Although the origin of the antimicrobial activity of fatty acids is still unclear, a general, widely accepted mechanism is that fatty acids physically disturb the microbial cellular membrane structure which results in increased fluidity and disorganization of the membrane followed by leaking of intracellular components and finally disintegration of the cells [20]. It was also suggested, using *Escherichia coli* (*E. coli*) as reference organism, that the increased penetration of ionic species across the disordered cell membranes might cause the lowering of the cytoplasmic pH and disruption of the redox balance, thereby inhibiting proliferation of the organism [21].

In this study, we prepare CPNs using octanoic acid (OA) as a surfactant in a polar medium via an emulsion process, fabricate composite films of CPNs and polyurethane (PU), and present both thermal storage and antimicrobial properties of the composites. Besides the antimicrobial activity of octanoic acid [21–23], it can be used as a surfactant to prepare nanoparticles of a non-polar hydrophobic conjugated polymer, poly[2,6-(4,4-bis-(2-ethylhexyl)-4*H*-cyclopenta[2,1-b;3,4-b′]-dithiophene)-*alt*-4,7-(2,1,3-benzothiadiazole)] (PCPDTBT), dispersed in a polar medium of *N*,*N*-dimethyl formamide (DMF) because its octyl chain can be closely associated with ethylhexyl side chains of PCPDTBT due to the comparable chain length (Scheme 1), which is demonstrated in the literature regarding optoelectronic devices [24] and biomedical applications [12]. Furthermore, CPNs contain carboxylic acid groups on their surfaces due to emulsification in polar media and can form hydrogen bonds with a representative fiber material, PU, thereby guaranteeing excellent compatibility and uniform distribution of the CPN fillers in the PU matrix. As a model system, we prepared CPNs and PU composite films and characterized their light absorption, heat generation, and antimicrobial properties. The novelty of our study is that the composite films can simultaneously show both of the photothermal [25] and antimicrobial effects [26] while maintaining their mechanical property due to a homogeneous distribution of filler nanoparticles in the matrix. For example, a representative antimicrobial material, silver nanoparticles (Ag NPs) can present both photothermal and antimicrobial properties. However, Ag NPs need to be closely assembled with each other in a matrix to enhance the photothermal effect by surface plasmon resonance which should deteriorate the mechanical properties of resulting composites.

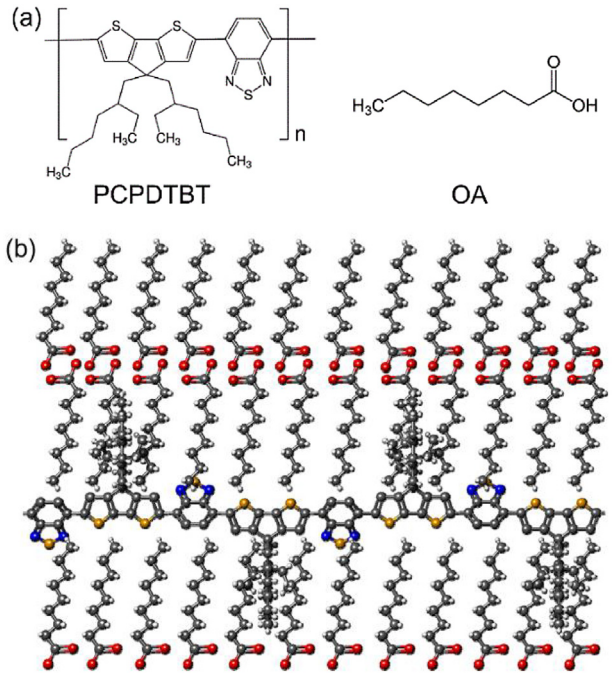

Scheme 1. (a) Chemical structures of PCPDTBT and octanoic acid (OA), and (b) schematic illustration of a molecular assembly between PCPDTBT and OA.

Experimental

Materials

PCPDTBT (MW = 34 kDa, PDI = 2.1, MW on a repeat unit basis = 534.845 g/mol, One Materials, Inc., Quebec, Canada), OA (MW = 144.21 g/mol, Sigma–Aldrich), PU (Estane® S TPU, Lubrizol Co., USA), and organic solvents (Sigma–Aldrich) were used as received.

Preparation of nano-ellipsoids, composite films and fibers

0.22 mL of OA solution (74 mg OA dissolved in 10 mL chloroform) was added to 20 mL of DMF under continuous stirring at 1500 rpm. After 15 min of stirring, 5 mL of PCPDTBT solution (1 mg PCPDTBT dissolved in 10 mL chloroform) was drop-wisely added and stirred for 1 h. The molar mixing ratio of PCPDTBT on a repeat unit basis to OA was 1:12 (0.94 μM PCPDTBT:11.29 μM OA). The solution was further ultrasonicated for 5 min and heated at 80 °C for 3 h under stirring at 1500 rpm to completely evaporate chloroform. To prepare PU:CPN composite films, PU was dissolved in DMF at 15 wt% and CPNs solutions in DMF were added to the PU solution under stirring at 1500 rpm. Mixture solutions of three different weight percentages (0.0, 0.25, 0.5, and 1.0 wt%) of CPNs to PU were prepared and poured into petri dishes, followed by drying in vacuum at 25 °C for two days. As a reference sample, silver nanoparticles (Ag NPs) were synthesized by adding an aqueous solution of silver trifluoroacetate into DMF. Then, the resulting solution was heated at 100 °C for 5 min to reduce the silver ions using DMF as both solvent and reducing agent. A detailed procedure can be found elsewhere [27]. Control samples of PU films composited with 1 wt% of OA and PCPDTBT were prepared by mixing the PU DMF solution (15 wt%, 0.4 g) with OA and PCPDTBT dissolved in DMF and chloroform, respectively, followed by drying onto petri dishes. The thicknesses of all prepared films were 120 μm as measured by a vernier calipers. Fibers of PU composited with 1 wt% CPNs were prepared by a conventional solution spinning process. The DMF solution of PU and CPNs was extruded through a syringe needle directly into a poor solvent, methanol, thereby precipitating the composite fibers. The resulting fibers were dried at room temperature in vacuum for overnight.

Characterization

UV–vis absorption spectra of the PCPDTBT nanoparticles were obtained with an ultraviolet–visible (UV–vis) spectrometer (V-670, JASCO, Japan). Morphological observations of the nanostructures were conducted on a field-emission scanning electron microscope (FE-SEM, SIGMA, Carl Zeiss, Germany) and a high resolution transmission electron microscope (HR-TEM, JEM3010, JEOL, Japan). Structural analysis using 2D grazing incidence X-ray diffraction (2D GIXD) was carried out at a synchrotron facility (6D

UNIST-PAL beamline of PLS-II at Pohang Accelerator Laboratory, Republic of Korea). Particle size analysis was performed by analyzing SEM images of CPNs using a GATAN Micrograph program. The photostability of PCPDTBT nano-ellipsoids dispersed in DMF was evaluated by monitoring the decrease in the maximum absorption intensity at every 15 min for 3 h under white light irradiation from a solar simulator (100 W, PEC-L01, Peccell Technologies Inc., Yokohama, Japan). An optical filter (400 nm cutoff, OD2 Longpass filter, Edmund Optics, New Jersey, USA) was used to cut off UV light when the photostability was measured under visible and near infrared (NIR) light. To estimate the photothermal storage properties, the PU-CNP films were positioned at a distance of 20 cm from the solar simulator and heat generation images were recorded by a NIR camera (FLIR, TG165, Japan) every 10 min for 1 h under white light irradiation and for the next 1 h after turning off the light irradiation. Optical and fluorescence images of composite fibers were recorded using a microscope (Olympus BX-51, Tokyo, Japan) with a Cy5 filter.

Antibacterial test

Antibacterial properties of blank (no films in dishes), pristine PU films, and PU composite films containing 1 wt% Ag NPs, or 0.25, 0.5, and 1.0 wt% CPNs were monitored using two kinds of bacteria, *Staphylococcus aureus* (*S. aureus*, ATCC 6538P, American Type Culture Collection, Manassas, VA, USA) and *E. coli* (*E. coli*, ATCC 8739, American Type Culture Collection, Manassas, VA, USA) by incubating the bacteria on films in petri dishes for 24 h at 35 °C. The average concentrations of *S. aureus* and *E. coli* immediately after inoculating the cells on blank dishes (M_a in colony forming unit/ml (CFU/ml)) and those after 24 h incubation (M_b) on the dishes were estimated as reference concentrations. On the other hand, the bacterial concentrations after incubation for 24 h on dishes with pristine PU films, composite films of PU containing 1 wt% Ag nanoparticles, and composite films containing 0.25, 0.5, and 1.0 wt % CPNs (M_c) were evaluated to estimate antibiosis behaviors of the composite samples.

$$\text{Antimicrobial activity (S)} = \log\frac{M_b}{M_c} \quad (1)$$

$$\text{Degree of concentration reduction (\%)} = \left[\frac{M_b - M_c}{M_b}\right] \times 100 \quad (2)$$

Results and discussion

Preparation of conjugated polymer nano-ellipsoids

CPNs were prepared in DMF, a solvent in which PU can be readily dissolved. Thus, composites of CPNs and PU could be formed by facile mixing of both components' DMF solutions. In our process, OA dissolved in chloroform was added to DMF under stirring, producing a clear solution. To this solution, a PCPDTBT chloroform solution was drop-wisely added at the PCPDTBT to OA molar mixing ratio of 1:12 and stirred for 1 h to form an emulsion. It should be mentioned that a phase separation between the OA DMF solution and the PCPDTBT chloroform solution could be observed when the stirring was stopped after 5 min, indicating that no emulsification had taken place. Because of the incompatibility of non-polar PCPDTBT and polar DMF, it is thought that PCPDTBT chloroform droplets are separated from DMF and that OA partitions both phases due to its amphiphilicity. The solubility of OA in DMF is low while OA is completely soluble in chloroform. Thus, it is thought that the polar ends of the carboxylic groups in OA are located at the interface between the PCPDTBT chloroform droplets and DMF. After the complete removal of chloroform upon heating, nano-ellipsoids of PCPDTBT are formed as shown in Fig. 1a. The average sizes of these nano-ellipsoids were found to be 298.5 ± 56.9 nm in the long axis and 119.5 ± 22.9 nm in the short axis of the nano-ellipsoids. A TEM image of the prepared CPNs also shows dark particulates that present conjugated polymers with high electron density (Fig. 1b).

Properties of conjugated polymer nano-ellipsoids

It is anticipated that the OA molecules are closely associated with the PCPDTBT chains due to packing between alkyl chains based on hydrophobic interactions during the removal of the organic solvent, and that the surfaces of CPNs contain carboxylic acid groups that face the polar DMF medium. The assembly structure of CPNs at the PCPDTBT to OA mixing ratio of 1:12 was examined by grazing-incidence X-ray diffraction technique after drop casting and drying of the CPN solution on a silicon substrate. The resulting 2D GIXD pattern and its out-of-plane line-cut (q_z-profile) in Fig. 2a and b, respectively, show a few hazy diffuse rings in a range of q = 1.2–1.7 $Å^{-1}$, indicating a randomly distributed assembly structures. However, diffraction spots that originate from closely assembled conjugated backbones with lateral packing of alkyl chains are clearly shown in the red-dashed box in Fig. 2a. Especially, the *d*-spacing of (*2h1*) diffractions at $q = 1.25$ is ~5.0 Å, which corresponds to closely associated lateral packing of conjugated planes as demonstrated in CPNs assembled with

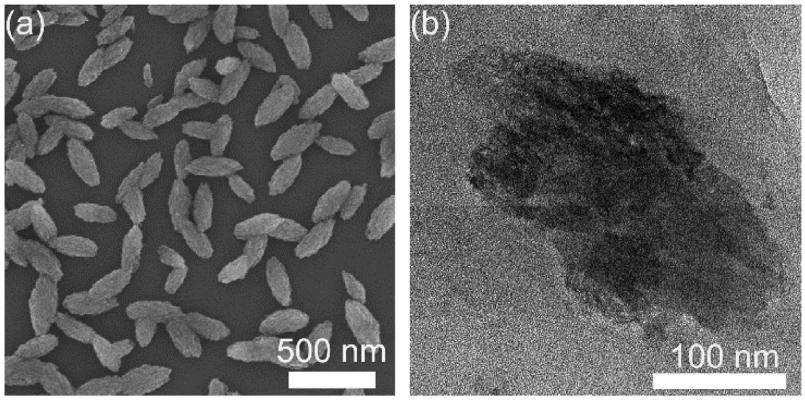

Fig. 1. (a) SEM image and (b) TEM image of PCPDTBT nanoellipsoids assembled with OA at the molar mixing ratio PCPDTBT to OA of 1:12.

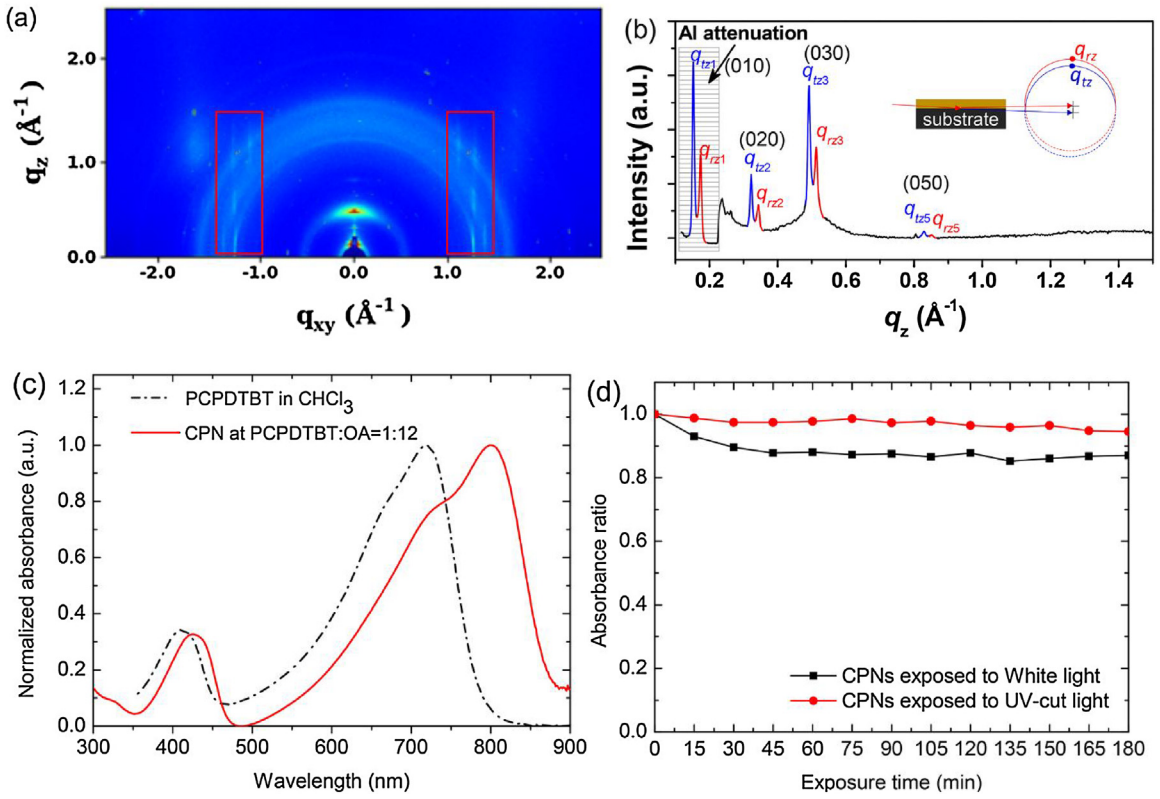

Fig. 2. (a) 2D GIXD pattern and (b) its out-of-plane line cut of PCPDTBT:OA nano-ellipsoids assembled at a 1:12 mixing ratio, where the series of q_{tz} and q_{rz} diffraction peaks are originated from the transmitted and reflected beam, respectively. (c) Absorption spectra of PCPDTBT:OA nanoparticles assembled at three different mixing ratios in comparison to that of only PCPDTBT dissolved in chloroform. (d) Decrease in the absorption maximum of PCPDTBT:OA nanoparticles prepared at 1:12 mixing ratio under white light irradiation for 3 h.

phospholipids [12,28] and alkylbenzoic acids [29]. Also, the 2D GIXD pattern and its line-cut profile clearly show (*0h0*) diffractions along the out-of-plane direction, where the (*010*) diffraction is attenuated by Al plate for the clear view of the higher order diffraction peaks with longer X-ray exposure time. It is noticeable that the (*0h0*) diffraction is extended up to the 5th order, although only a trace remains in the (*040*) diffraction peak. The *d*-spacing and coherence length (apparent crystallite size) calculated by the peak width of (*010*) diffraction is 36.6 Å and ~76 nm, respectively, which suggests the nano-ellipsoids are composed of ~20 layers with 36.6 Å unit layer along the out-of-plane direction. These results indicate a bi-layered structure, in which PCPDTBT chains are assembled with a bilayer of OA because the *d*-spacing of the (*010*) diffraction corresponds to the summed length of a PCPDTBT layer and bilayer of fully extended OA molecules. In general, an emulsification process for assembling conjugated polymers with surfactants produces spherical particulates because the lateral alkyl chain packing by hydrophobic interactions and surface tension minimization overwhelm the stacking of conjugated planes due to π–π interactions [30]. Interestingly, our emulsion process using octanoic acid produces ellipsoids, presenting the contribution of hydrogen bonds by carboxylic acids to the enhanced growth of molecular assemblies in the long axis.

PCPDTBT chains closely assembled with OA provide enhanced optical properties to the resulting CPNs. When PCPDTBT is dissolved in chloroform as single chains, its absorption maximum appears at 718 nm, reflecting intramolecular electron delocalization of the conjugated backbones. In comparison, CPNs of PCPDTBT and OA show their absorption maximum at 799 nm as shown in Fig. 2c. This strong bathochromic shift originates from closely packed conjugated backbones in assemblies with alkyl chains of OA. Similar bathochromic shift in assemblies with amphiphiles such as phospholipids and resulting intermolecular electron delocalization was proven by our density functional theory calculations [31]. With this strongly enhanced absorption in the near infrared range, the photostability of the resulting CPNs in DMF solution is significantly enhanced as demonstrated by monitoring the decrease in absorption maximum at 799 nm under white light and cutting off ultraviolet light irradiation generated by a solar simulator (Fig. 2d). After 3 h of irradiation under white light and visible/NIR light excluding UV frequencies, the absorption maxima decreased down to 87.0 and 94.5% of their initial intensity, respectively. In comparison, the absorption maxima of CPNs prepared from a nanoprecipitation process, in which PCPDTBT chains in a diluted chloroform solution are precipitated in excess methanol upon dropwise addition without using any surfactant, decreased to 73.4 and 83.0% of their original intensity for the irradiation under white light and visible/NIR light excluding UV frequencies, respectively [29]. These results show that PCPDTBT chains closely assembled with OA can be protected from the attack of active species in the surrounding medium, such as active radical or ions generated upon light irradiation, and that CPNs of PCPDTBT:OA assemblies can be attractive fillers for compositing with fiber materials.

Properties of PU films composited with conjugated polymer nano-ellipsoids

Because CPNs are prepared as dispersion in DMF that can strongly solvate PU and contain carboxylic acid groups on their surfaces, composites of PU and CPNs can be formed simply by mixing both DMF solutions and subsequent solvent removal. In Fig. 3a, a SEM image of the PU composite surface containing 1 wt% CPNs shows uniformly distributed CPNs on the composite surface

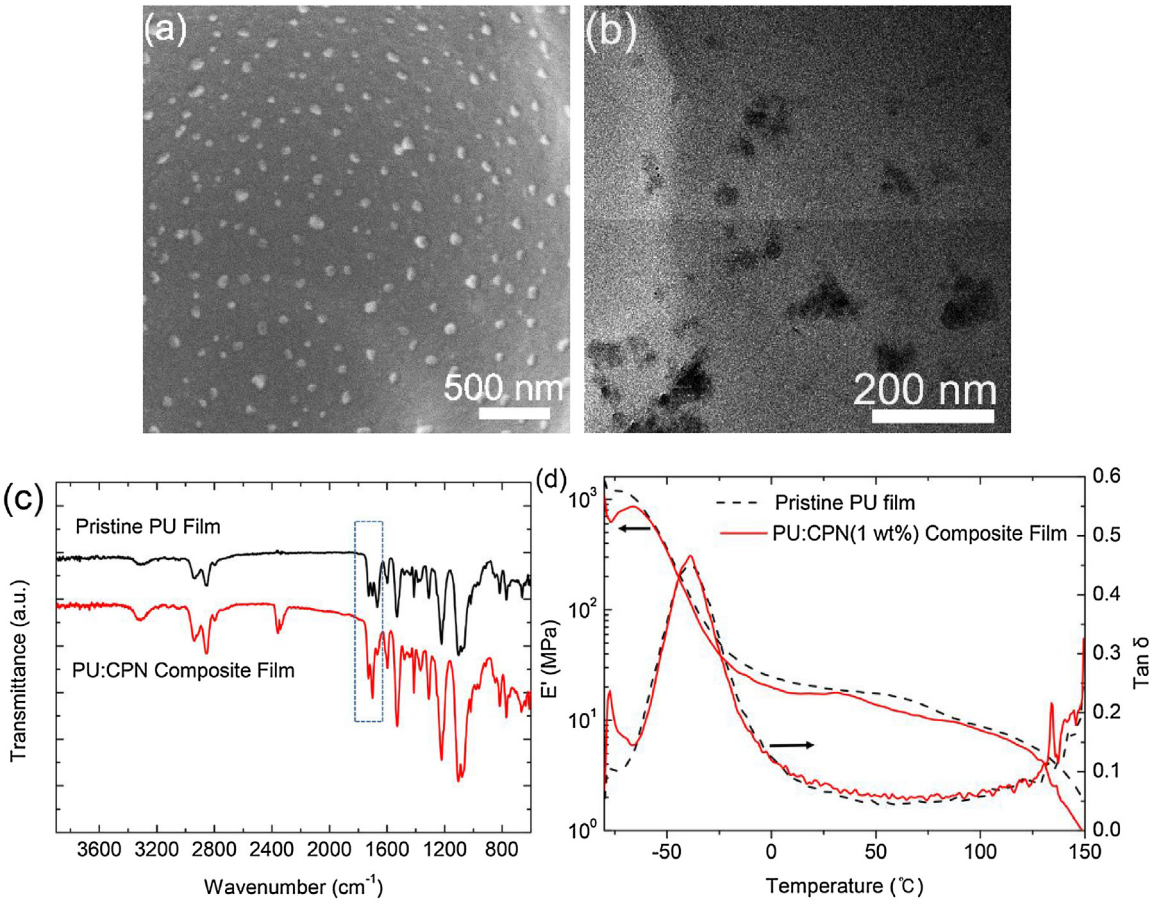

Fig. 3. (a) SEM and (b) cross-sectional TEM images of PU:CPN (1:12) composite films containing 1 wt% of CPNs. (c) FT-IR spectra and (d) dynamic mechanical analysis data of pristine PU and PU:CPN composite films.

although nano-ellipsoids are further broken to smaller particulates during mixing. In this image, CPNs appear as bright dots due to their high electron density. The cross-sectional TEM image displayed in Fig. 3b also shows the uniform distribution of CPNs as dark particulates in the PU matrix. The existence of carboxylic acid groups and hydrogen bonds were confirmed by FT-IR spectroscopy as shown in Fig. 3c. Pristine PU films show a characteristic IR band for hydrogen bonded secondary amine (−NH) in urethane units at around 3315 cm^{-1} [32]. Also, IR bands of non-hydrogen bonded carbonyl at 1730 cm^{-1} and hydrogen bonded carbonyl in urethane units at 1700 cm^{-1}, and carbonyl in urea units at 1664 cm^{-1} located in the dashed box of Fig. 3c clearly indicate partial hydrogen bonds between urethane units and the existence of urea units in the PU film as side products [33]. After compositing PU with 1 wt% of CPNs, both the hydrogen bonded carbonyl band at 1700 cm^{-1} and the secondary amine band at around 3315 cm^{-1} significantly increase as clearly shown in Fig. 3c, indicating enhanced hydrogen bonding between urethane units in PU and the surface carboxylic acid groups of CPNs. As for mechanical properties, the thermal transition of the tensile storage modulus (E') and the loss tangent for the pristine PU film and the PU:CPN composite film in the temperature range of −80 to 150 °C were measured by dynamic mechanical analysis to examine any deterioration of mechanical properties of PU after compositing

Table 1
Antibacterial activity and reduction of bacteria concentrations pristine PU and composites with Ag nanoparticles, PCPDTBT and CPNs.

	Sample	M_a (CFU/mL)	M_b (CFU/mL)	M_c (CFU/mL)	Antibacterial activity (S)	Reduction of bacteria (%)
S. aureus	PU	2.1×10^5	1.0×10^7	7.3×10^6	0.1	27.3
	PU:OA (1.0 wt%)	2.3×10^5	1.1×10^7	10	6.0	99.9
	PU: Ag NP (1.0 wt%)	2.1×10^5	1.0×10^7	<10	6.0	99.9
	PU:PCPDTBT (1.0 wt%)	2.3×10^5	1.1×10^7	6.4×10^5	1.2	94.2
	PU:CPN (0.25 wt%)	2.2×10^5	1.0×10^7	1.7×10^6	0.8	83.2
	PU:CPN (0.5 wt%)	2.2×10^5	1.0×10^7	<10	6.0	99.9
	PU:CPN (1.0 wt%)	2.1×10^5	1.0×10^7	<10	6.0	99.9
E. coli	PU	2.3×10^5	1.1×10^7	7.2×10^6	0.1	34.7
	PU:OA (1.0 wt%)	2.4×10^5	1.3×10^7	<10	6.1	99.9
	PU: Ag NP (1.0 wt%)	2.3×10^5	1.1×10^7	<10	6.0	99.9
	PU:PCPDTBT (1.0 wt%)	2.4×10^5	1.3×10^7	4.0×10^6	0.5	68.9
	PU:CPN (0.25 wt%)	2.2×10^5	1.0×10^7	2.1×10^6	0.7	80.8
	PU:CPN (0.5 wt%)	2.2×10^5	1.0×10^7	<10	6.0	99.9
	PU:CPN (1.0 wt%)	2.3×10^5	1.1×10^7	<10	6.0	99.9

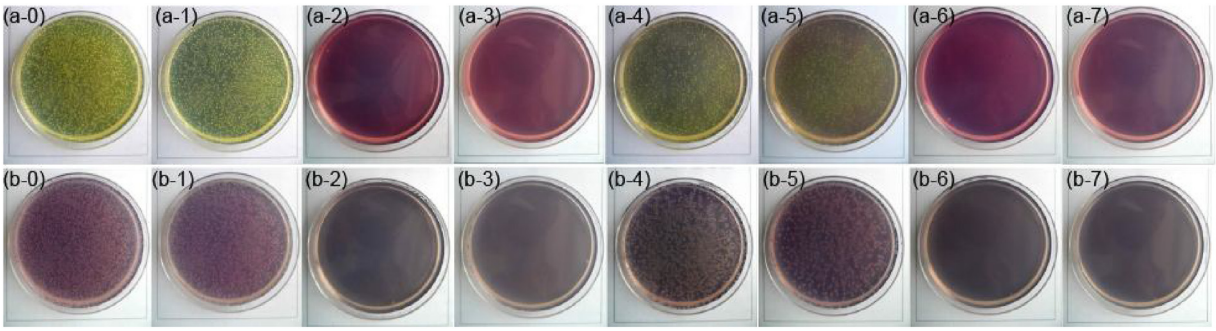

Fig. 4. Antibacterial activity analysis of (a) *S. aureus* and (b) *E. coli* for (0) blank samples, (1) pristine PU film, PU composite films with (2) 1 wt% OA, (3) 1 wt% Ag nanoparticles, (4) 1 wt% PCPDTBT, (5) 0.25 wt%, (6) 0.50 wt% and (7) 1.0 wt% CPNs.

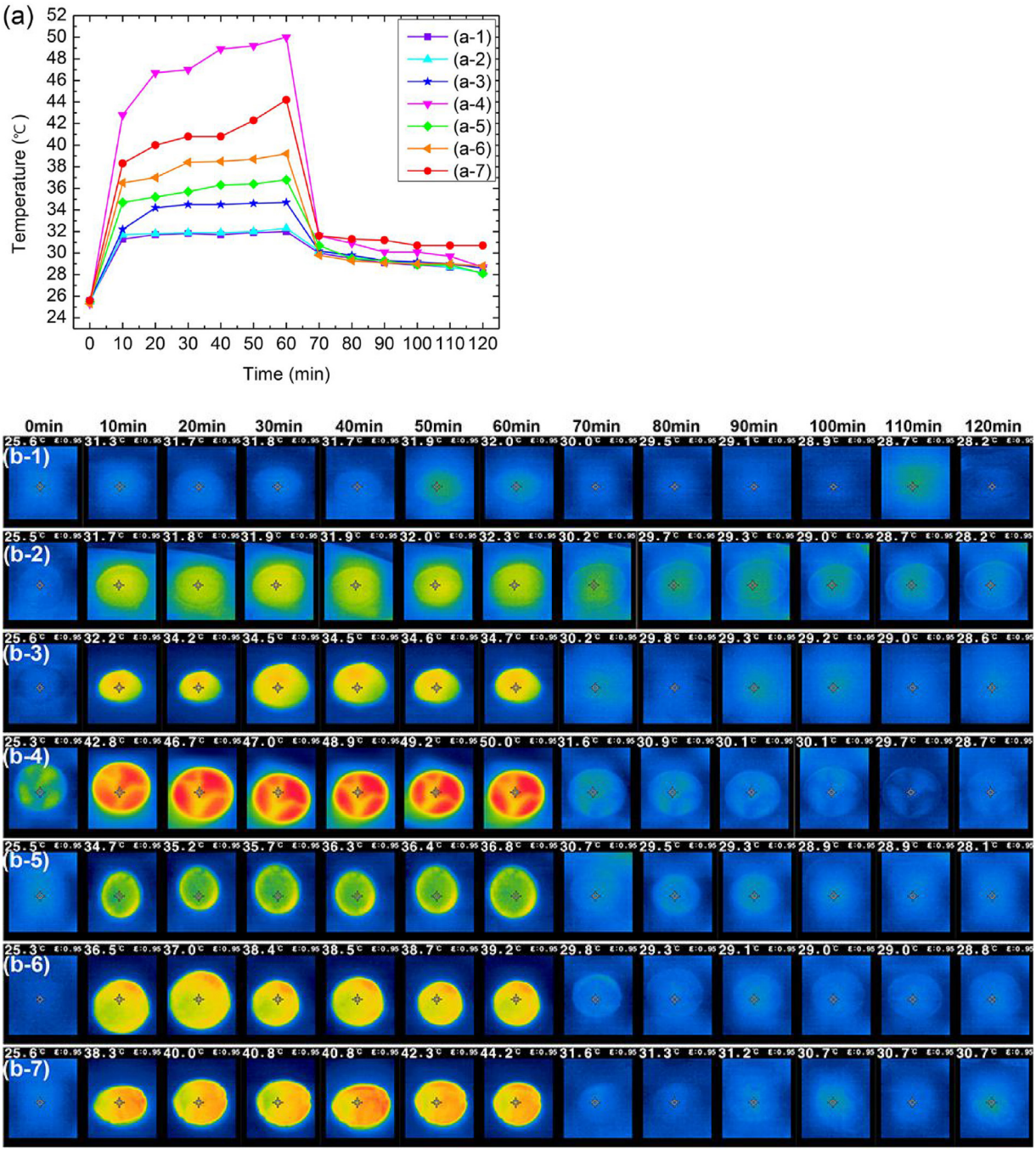

Fig. 5. (a) Temperature variation profiles and (b) NIR images under white light irradiation for 60 min and after turning off the light for the following 60 min for (1) pristine PU film, PU composite films with (2) 1 wt% OA, (3) 1 wt% Ag nanoparticles, (4) 1 wt% PCPDTBT, (5) 0.25 wt%, (6) 0.50 wt% and (7) 1.0 wt% CPNs.

with CPNs. In the plot of the loss tangent, both films exhibit identical β relaxations at −38 °C that correspond to soft segment relaxations in the PU. The storage modulus values of both films were in the order of GPa below the β relaxation, drastically decreased to a few tens MPa above the β relaxation, and nearly reached to zero at 150 °C, which show a typical behavior of thermoplastic elastomers. Remarkably, the difference in storage modulus values between the pristine PU film and the PU:CPN composite film were less than 5 MPa in the temperature range of 0–150 °C, presenting only slight deterioration of mechanical properties after compositing with CPNs.

Antimicrobial and photothermal properties of PU nanocomposites

The antibacterial activity of PU:CPN composite films was examined as a model system for PU:CPN fibers. The results summarized in Table 1 and Fig. 4 present the antibacterial activity of PU:CPN composite films comparable to a PU:silver nanoparticle (Ag NP) composite film that contains conventional, popular antimicrobial Ag NPs. The pristine PU films show the lowest antibacterial activity and reduction of bacterial concentrations, which are 0.1 and 27.3%, respectively. When PU is composited with 1 wt% Ag NP, the antibacterial activity dramatically increased to 6, and 99.9% of *S. aureus* and *E. coli* were eliminated after 24 h incubation at 35 °C on the film, presenting an excellent antibacterial effect as well described previously in the literature [34–37]. PU:CPN films at two different mixing ratios of 0.5 and 1.0 wt% showed identical antibacterial activity and reduction of bacterial concentration as the PU:Ag NP composite while the PU:CPN composite at 0.25 wt% was inferior to the PU:Ag NP composite in activity and concentration reduction, which were 0.7 and 80.8%, respectively. However, it should be noted that a smaller amount of CPNs than Ag NPs is required to provide identical antibacterial properties of the composite. The use of OA should play a key role on the antimicrobial activity of the PU composites. When we prepared PU films composited with 1 wt% of OA and PCPDTBT, the PU:OA composite film presented the excellent antibacterial activity and reduction percentage of bacteria comparable to the PU:AgNP composite film. However, PU:PCPDTBT film show 1.2 and 94.2% of the antibacterial activity and reduction of bacteria, respectively for *S. aureus* and 0.5 and 68.9% for *E. coli*. These results explicitly indicate that the antimicrobial activity of PU:CPN composites comparable to that of PU:AgNP originates from the use of OA.

In the thermal storage analysis summarized in Fig. 5, PU composite films with 1 wt% PCPDTBT and PU:CPN composite films at all CPN concentrations of 0.25, 0.5, and 1.0 wt% show higher temperature increases than the pristine PU film and the PU films composited with 1 wt% OA and Ag NPs when they are exposed to white light from a solar simulator for 1 h. After 1 h of irradiation, the temperatures in the middle of the films exposed to the light were 50.0, 44.2, 39.2, 36.8, 34.7, 32.3 and 32.0 °C for PU composites with 1 wt% PCPDTBT, 1.0, 0.5, and 0.25 wt% CPNs, 1 wt% Ag NPs, 1 wt % OA, and pristine PU, respectively. Thus, PU:CPN composites using smaller amounts of CPNs emit more thermal energy after light absorption than the PU:Ag NP composite. Furthermore, our results show that the PU:CPN composite with 1 wt% CPNs still stores thermal energy, as indicated by its higher temperature of 30.7 °C, after turning off the solar simulator than the other samples, all of which were below 28.8 °C.

The applicability of PU composited with 1 wt% CPNs to fibers was investigated by preparing a model fiber via a solution spinning process using a syringe. In the resulting composite fibers with a diameter of about 250 μm, CNPs were distributed without agglomeration as when in Fig. 6a. The uniform distribution of CPNs in the PU matrix was further confirmed by measuring its fluorescence image with a Cy5 filter. As shown in the optical and

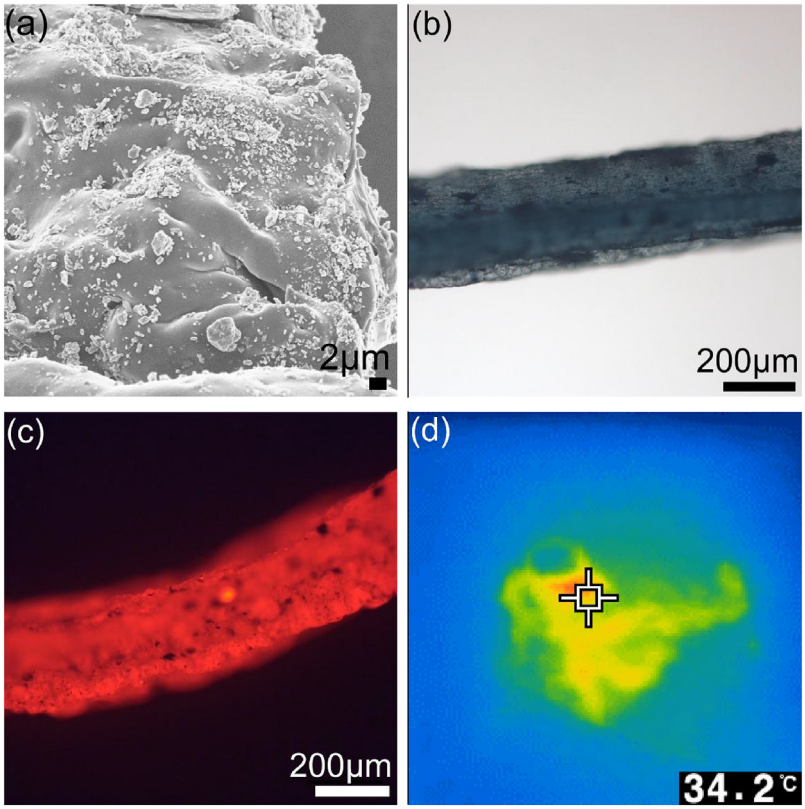

Fig. 6. PU fiber composited with 1.0 wt% CPNS: (a) FE-SEM, (b) optical, (c) fluorescence (excitation wavelength = 650 nm) and (d) NIR images after white light irradiation for 60 min.

fluorescence images in Fig. 6b and c, strong red fluorescence presents the existence of uniformly dispersed CPNs. The fiber also has the photothermal effect as shown in the NIR image taken after white light irradiation for 60 min (Fig. 6d).

Conclusion

In summary, nano-ellipsoids of conjugated polymers were prepared in DMF via an emulsion process using the fatty acid OA as an emulsifier and a polymer solution in chloroform as an organic phase. Upon removal of the organic solvent by heating, CPNs were produced. From a view point of fiber or film processing, DMF solutions of CPNs facilitate complete mixing with DMF solutions of a conventional fiber material, such as PU, thereby enabling film or fiber formation upon solvent removal. Also, surface carboxylic acids on the surface of the CPNs induce hydrogen bonds with urethane units in PU, thereby guaranteeing a uniform distribution of CPNs in the PU matrix. Photothermal and energy storage properties of CPNs and the antibacterial activity of the fatty acids can provide synergetic multifunctionalities to fiber materials.

Acknowledgements

The authors thank to Seong-Hun Lee and Juhyun Yang, who have helped GIXD experiments. This research was financially supported by grants from the National Research Foundation of Korea (Grant No. NRF-2017R1E1A2A02023491 and 2017R1A2B4005315). Experiments at PLS-II 6D UNIST-PAL beamline were supported in part by MSIT, POSTECH, and UCRF.

References

[1] S.R. Wickramasinghe, M.J. Semmens, E.L. Cussler, J. Membr. Sci. 84 (1993) 1.
[2] J.W. Yoon, Y. Park, J. Kim, C.H. Park, Fash. Text. 4 (2017) 9, doi:http://dx.doi.org/10.1186/s40691-017-0090-4.
[3] Y. Huang, H. Hu, Y. Huang, M. Zhu, W. Meng, C. Liu, et al., ACS Nano 9 (2015) 4766.
[4] Y.S. Nam, X.M. Cui, L. Jeong, J.Y. Lee, W.H. Park, Thin Soild Films 517 (2009) 6531.
[5] P. Schwarzkoff, R. Kieffer, Refractory Hard Metals: Borides, Carbides, Nitrides and Silicides, The Macmillan Company, New York, 1953.
[6] X.M. He, L. Shu, H.B. Li, D. Weng, J. Mater. Res. 14 (1999) 615.
[7] G.H. Reynolds, J.C. Janvier, J.L. Kaae, J.P. Morlevat, J. Nucl. Mater. 62 (1976) 9.
[8] B.V. Cockeram, D.P. Measures, A.J. Mueller, Thin Solid Films 355–356 (1999) 17.
[9] S. Mondal, Appl. Therm. Eng. 28 (2008) 1536.
[10] J.A. Lemire, J.J. Harrison, R.J. Turner, Nat. Rev. Microbiol. 11 (2013) 371.
[11] G. Dhiman, J.N. Chakraborty, Fash. Text. 2 (2015) 13, doi:http://dx.doi.org/10.1186/s40691-015-0040-y.
[12] J. Yoon, J. Kwag, T.J. Shin, J. Park, Y.M. Lee, Y. Lee, et al., Adv. Mater. 26 (2014) 4559.
[13] J. Geng, C. Sun, J. Liu, L.D. Liao, Y. Yuan, N. Thakor, J. Wang, B. Liu, Small 11 (2014) 1603.
[14] C. Kim, S.Y. Kim, Y.T. Lim, T.S. Lee, Macromol. Res. 25 (2017) 572.
[15] K. Pu, A.J. Shuhendler, J.V. Jokerst, J. Mei, S.S. Gambhir, Z. Bao, J. Rao, Nat. Nanotechnol. 9 (2014) 233.
[16] L. Cui, J. Rao, WIREs, Nanomed. Nanobiotechnol. 9 (2017) e1418, doi:http://dx.doi.org/10.1002/wnan.1418.
[17] J. Park, J. Ind. Eng. Chem. 51 (2017) 27.
[18] M. Liras, M. Iglesias, F. Sanchez, Macromolecules 49 (2016) 1666.
[19] N.M. Carballeira, Prog. Lipid Res. 47 (2008) 50.
[20] V. McDonough, J. Stukey, T. Cavanagh, Biochim. Biophys. Acta 2002 (1581) 109.
[21] M. Rodriquez-Moya, R. Gonzalez, J. Proteom. 122 (2015) 86.
[22] C.B. Huang, Y. Alimova, T.M. Myers, J.L. Ebersole, Arch. Oral Biol. 56 (2011) 650.
[23] Y.J. Guo, Z.Z. Pan, C.Q. Chen, Y.H. Hu, F.J. Liu, Y. Shi, J.H. Yan, Q.Z. Chen, Appl. Biochem. Biotechnol. 162 (2010) 1564.
[24] J. Peet, J.Y. Kim, N.E. Coats, W.L. Ma, D. Moses, A.J. Heeger, G.C. Bazan, Nat. Mater. 6 (2007) 497.
[25] K.-S. Lee, M.A. El-Sayed, J. Phys. Chem. B 110 (2006) 19220.
[26] M. Rai, A. Yadav, A. Gade, Biotechnol. Adv. 27 (2009) 76.
[27] I. Pastoriz-Santos, M. Liz-Marzán, Langmuir 15 (1999) 948.
[28] Y.K. Choi, D. Lee, S.Y. Lee, T.J. Shin, J. Park, D.J. Ahn, Macromolecules 50 (2017) 6935.
[29] N. Bae, H. Park, P.J. Yoo, T.J. Shin, J. Park, J. Ind. Eng. Chem. 51 (2017) 172.
[30] L. Zang, Y. Che, J.S. Moore, Acc. Chem. Res. 41 (2008) 1596.
[31] D. Seo, J. Park, T.J. Shin, P.J. Yoo, J. Park, K. Kwak, Macromol. Res. 23 (2015) 574.
[32] F. Mutsuhisa, K. Ken, N. Shohei, Polymer 487 (2007) 997.
[33] I. Clemitson, Castalble Polyurethane Elastomers, Taylor & Francis Group, New York, 2008.
[34] J.S. Kim, E. Kuk, K.N. Yu, J.H. Kim, S.J. Park, H.J. Lee, et al., Nanomedicine 3 (2007) 95.
[35] T.S. Kim, J.R. Cha, M.S. Gong, Macromol. Res. 25 (2017) 856.
[36] H. Madhav, P. Singh, N. Singh, G. Jaiswar, Macromol. Res. 25 (2017) 689.
[37] C.S. Shivananda, S. Asha, R. Madhukumar, S. Satish, B. Narayana, K. Byrappa, Y.J. Wang, Y. Sangappa, Macromol. Res. 24 (2016) 684.